OPEN-SOURCE PARALLEL CODES FOR 2D AND 3D FLOW SIMULATION BY LAGRANGIAN VORTEX METHODS

ILIA MARCHEVSKY, EVGENIYA RYATINA, GEORGY SHCHEGLOV & KSENIIA SOKOL
Bauman Moscow State Technical University, Russia

ABSTRACT

Meshless Lagrangian vortex methods that are characterized by considering vorticity as a primary computational variable are discussed, including their modern modifications for 2D and 3D flow simulation. Original mathematical models developed by the authors are described, that allow for significant improvement of the accuracy of the flow simulation around the airfoils/bodies. The hierarchy of numerical schemes based on the Galerkin approach is developed for numerical solution of the boundary integral equation. The quality of the surface mesh is not essential, rather high quality of the numerical solution can be achieved even for low-quality mesh consists of triangular cells with high aspect ratio. The open-source parallel codes (for CPU and GPU, using OpenMP, MPI and Nvidia CUDA technologies) are developed, that implement viscous vortex domains method and closed vortex loops method for 2D and 3D cases, respectively In 3D cases, the numerical scheme allows to satisfy the divergence-free condition for vorticity field (in 2D it is done trivially). The suggested methods can be applied for unsteady hydrodynamic load computation at rather low computational cost of the algorithm. The developed models and algorithms are suitable for numerical simulation in coupled problems, including for light movable bodies. Both weakly-coupled and strongly-coupled strategies are implemented, the last one requires several iterations; at each of them the boundary integral equation is solved. In addition to flow simulation and hydrodynamic load estimation, the suggested technique allows for added masses tensor calculation with high accuracy. Efficient fast method of quasilinear numerical complexity, both well-known and developed by the authors for the integral equation solution and vortex particles (that simulate the vorticity distribution in the flow domain) evolution simulation are discussed. A number of numerical examples are presented, being performed for validation of the developed mathematical models, numerical algorithms and parallel codes.

Keywords: incompressible flows simulation, open-source code, FSI problems, OpenMP, MPI, Nvidia CUDA.

1 INTRODUCTION

Vortex methods of computational fluid dynamics are based on considering the vorticity as a primary computational variable and they belong to a class of pure Lagrangian particle-based methods or have hybrid Lagrangian–Eulerian nature.

The basic idea of vortex methods, at least in the 2D case is connected with fundamental result, that have been established by Professor N. E. Zhukovsky in 1906: if one considers velocity field in inviscid incompressible flow around some airfoil, then this field would coincide exactly with the velocity field, that is induced by incident flow and the influence of vortex sheet of some intensity, placed on the surface line of the airfoil. Thus, the airfoil can be replaced with a vortex sheet, and for its intensity determination either analytic or numerical approaches are used. When a separate airfoil of a simple shape is considered in the unbounded flow domain, a conformal mappings technique can be applied (elliptic airfoil, semi-circular airfoil, Zhukovsky wing airfoil and some others). For more complicated shapes the problems are reduced to solving the boundary integral equation, which can be of Fredholm-type (with bounded kernel), singular (with Cauchy/Hilbert-type kernel, the integral is understood in the sense of its principal value) or hypersingular (in Hadamard sense). A

WIT Transactions on Engineering Sciences, Vol 135,
www.witpress.com, ISSN 1743-3533 (on-line)
doi:10.2495/BE460151

number of numerical schemes are developed, which provide a different level of accuracy and complexity. The most popular and most well-known schemes follow from solving of Laplacian/Helmholtz equation with respect to potential, with the boundary conditions of the second kind, i.e., the Neumann problem: the normal derivative of the potential should be equal to some given function on the airfoil surface. Considering the solution in the form of the double-layer potential, one can easily derive the corresponding hyper-singular integral equation of the first kind.

However, there is no need to find the double layer density potential Φ as such, instead of it vortex sheet intensity can be considered, that is mathematically equal to the surface gradient of Φ, multiplied by normal unit vector: $\vec{\gamma} = \vec{n} \times (\nabla \Phi)$. Applying the necessary tricks, the equation is reduced (in 2D case) to singular one, that is solved in most known implementations of vortex methods.

At the same time, the other approach was suggested in Kempka et al. [1], that allows for considering a Fredholm-type equation of the second kind with respect to vortex sheet intensity: instead of boundary condition for normal component of velocity (that is equal to the normal derivative of the potential in the framework of potential flow), the condition for the tangent component of velocity is considered. For smooth airfoils, the kernel of the resulting equation is bounded, for airfoils with corner points or sharp edges the kernel is unbounded, but the corresponding integrals are understood in traditional sense (as improper ones).

Note, that the briefly described mathematical model can be generalized and used not only for solving the problems for inviscid flow (described by Euler equations), but also for viscous flows simulation, i.e., the Navier–Stokes equation solution, both in 2D and 3D cases. In the 3D case, the idea remains the same: vortex sheet intensity, which is now not scalar, but vector lying in tangent plane, is considered as unknown, and a vectoral boundary integral equation (BIE) of the second kind is solved, that expresses the boundary condition for the tangent velocity component. Such an approach is more efficient than the well-known approach [2] for constructing BIE of the first kind that expresses the boundary condition for the normal velocity component for which numerical schemes such as the scheme of discrete vortex method and some others are developed (*N*-schemes).

For solving BIE of the second kind the family of numerical schemes, for 2D and 3D simulations, based on the briefly described approach and Galerkin projection method, is called '*T*-schemes' ('*T*' means 'Tangent') [3]. Their usage in flows simulation seems to be essential: in the 2D case of viscous flows simulations, it is necessary to provide a high quality of velocity field reconstruction in the near-body area (in the boundary layer). Note, that for viscous flow vorticity flux is simulated from the body surface to the flow; according to Lighthill's approach, not attached, but a free vortex sheet is introduced, vorticity from it is discretized into a large number of small vortex particles, that move in the flow domain and form boundary layer and vortex wake. Stochastic and deterministic algorithms for simulation of such type are known: random walk method (RWM) [4], particle strength exchange (PSE) method [5], vorticity redistribution method (VRM) [6] and viscous vortex domains method (VVD) [7]. Namely, the VVD will be used in this work.

In 3D case there is no known purely Lagrangian methods; the review of known approaches can be found in Mimeau and Mortazavi [8]; let us focus only on vorticity generation procedure on the body surface. We suggest to use the vortex loops method, according to which vorticity in the flow domain is represented as closed structures: each loop is considered as closed vortex tube of small radius, which is generated on the body surface, and then moves in the flow. All vortex tubes have equal intensity (circulation), that makes it possible to simulate their merging, reconnections, etc. Initial positions of vortex loops coincide with level-set lines of double-layer potential density on the body surface, however, the results are much more accurate if the following strategy is used: firstly, the BIE is solved with respect to vortex sheet (using the *T*-scheme), and secondly, the potential density is reconstructed by using the least squares method. This two-steps scheme normally provides much better result in comparison to 'direct' hyper-singular BIE solution with respect to the potential density, especially for low-quality surface meshes.

2 BRIEF REVIEW OF EXISTING CODES

Despite the fact, that vortex methods have a long history [9], [10] dating back to the 1930s…1950s, up to now there are just a few software implementations, which are freely available for researchers, based on actual mathematical models and allows to use modern computational technologies (we do not take in mind the so-called 'panel methods', implemented in some codes, since they can be considered only as a very simple modification of vortex methods, that is suitable for some specific problems). Some codes have appeared in recent years; let us confine ourselves to listing them without detailed description of their capabilities.

The vvflow [11] (available from 2018) is based on the VVD method and allows to simulate for 2D flow. Coupled FSI problems can be considered for rigid elastically connected airfoils. For computations only OpenMP technology is used; so it can be run on multicore processors with shared memory; CUDA is not supported.

Codes Omega2D [12] and Omega3D [13] have appeared in 2018, they are based on VRM method. Only flow around immovable airfoils/bodies can be simulated; however, the codes are developed intensively, e.g., in 2022 the fast algorithm (of Barnes–Hut type) is implemented for vortex particle influence computation. Parallel computational technologies are not used 'explicitly', however, OpenMP and CUDA can be 'implicitly' used through the third-party libraries.

In 2019, the FLOWVPM code have appeared as a part of the FLOWUnsteady project [14]. 3D flows around bodies, fixed and movable, are considered. Vortex blobs are considered as vortex particles; note, that in this code fast multipole method (FMM) used for vortex particle influence computation, however parallel computational technologies are not widely used.

It is also known about the VXflow code [15], which is used actively by developers, however, it is not freely available. This code is for 2D problems; it is based on RWM approach [4] and the fast Fourier transform (FFT) technique for vortex particles interaction simulation. Algorithms for parallelization are based on OpenCL technology, so some part of computations can be transferred to a graphic card.

In all mentioned codes traditional approach is used for the boundary condition satisfaction: singular or hyper-singular BIE is solved, usually by using rather coarse numerical schemes.

3 THE VM2D AND VM3D CODES

Since the freely available codes now are based on outdated mathematical models and in most cases do not allow using modern high-performance computational technologies, the authors developed original implementations of vortex methods (VM) for 2D and 3D cases, based on *T*-schemes, VVD (in 2D) and closed vortex loops method (in 3D), and intensive use of capabilities of both multicore/multiprocessor computers and modern graphic cards. The source code of VM2D is open and freely available in GitHub public repository:

http://github.com/vortexmethods/VM2D (accessed on 26 Jun. 2023); the VM3D code will be available soon.

The general flowchart of both algorithms is shown in Fig. 1; there are no principal differences in blocks of VM2D and VM3D, however, most parts of specific algorithms differ significantly.

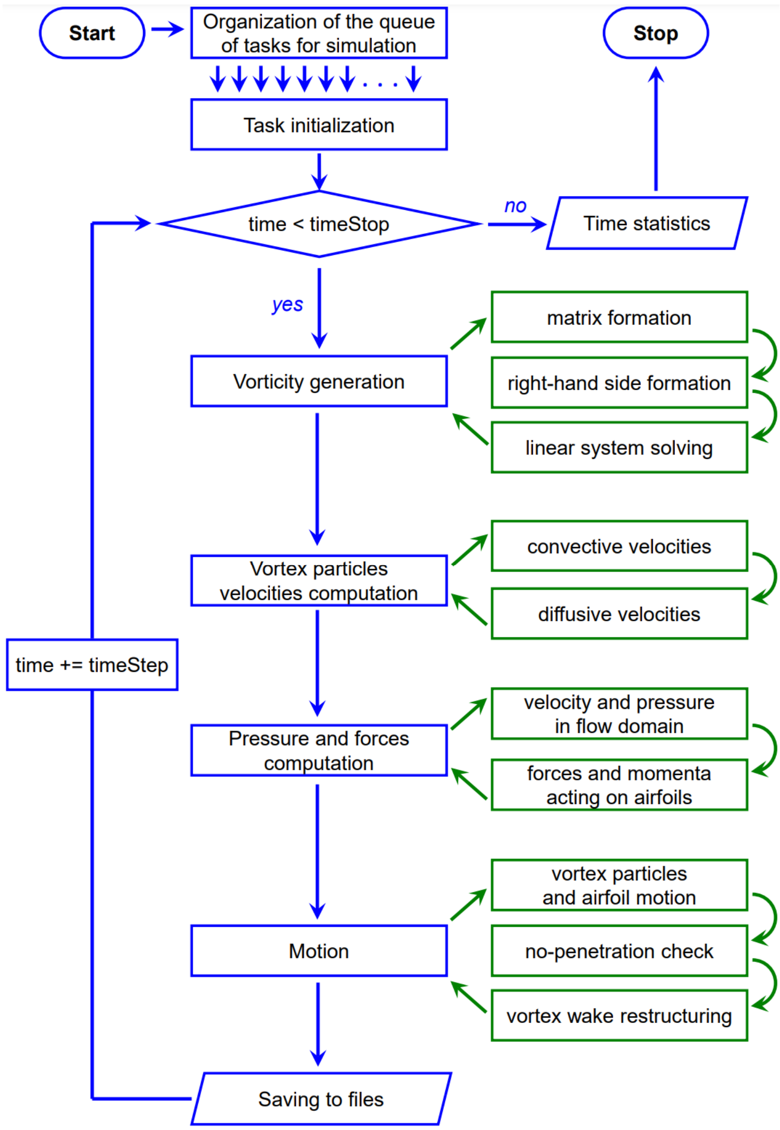

Figure 1: Flowchart of vortex method algorithm.

Codes are written in C++ language, cross-platform and have a modular structure. Parallel technologies OpenMP, MPI and Nvidia CUDA are used for performing computations on shared memory systems, distributed memory cluster systems and graphic accelerators, respectively.

To improve the efficiency of computations performed on CPU, at least for the most time-consuming computational blocks of the algorithm (particle velocities computation and BIE solving) it is reasonable to use special fast algorithms. Such an algorithm is developed as prototypes and applied for both mentioned problems: it is a hybrid Barnes–Hut/multipole algorithm, that has of quasilinear computational complexity [16], [17]. Its implementation is rather efficient, it allows to achieve speedup of about 1,800 times for the velocities computation of 2 million vortex particles in parallel mode (OpenMP, 18 cores). The time of BIE solving for elliptical airfoil discretized by $N = 3{,}200$ panels at one time step is reduced by 50 times in comparison with the Gaussian elimination algorithm for the corresponding system of linear equations.

However, in the current version of open codes only direct algorithms are implemented (fast algorithms will be available in the nearest future). It means that in order to reduce computation time it is necessary to use a lot of CPU cores or graphics accelerators. To estimate the efficiency of parallel implementation of VM2D code for the problem of flow simulation around a circle airfoil, which is discretized by $N = 2{,}000$ panels, is considered at Re = 3,000. Computations are performed on the cluster with 84 nodes, each is equipped with 28 cores (2xIntel Xeon E5-2690v4). The efficiency of parallel implementation is about 70% for fixed time-step with approximately 600 000 vortex particles in the vortex wake. It corresponds to 0.45% of sequential code, according to the Amdahl's law. Since the vortex method is a particle method, and all the particles can be processed independently, its parallel implementation adapted for calculations using graphics accelerators is extremely efficient: computational time of one time-step with 600,000 vortex particles by using a single GPU Tesla V100 is approximately the same as using 84 nodes, each with 2 × 14-core CPU.

4 NUMERICAL RESULTS

4.1 Unsteady hydrodynamic loads computation for impulsively started cylinder

In the VM2D code for the BIE solution the T-schemes with piecewise-constant and piecewise-linear solution representation are implemented for rectilinear panels that discretize airfoil surface line. In order to verify the developed T-schemes for the boundary integral equation solution the well-known test problem of flow simulation around an impulsively started circular cylinder is considered at the Reynolds number Re = 200 (Fig. 2).

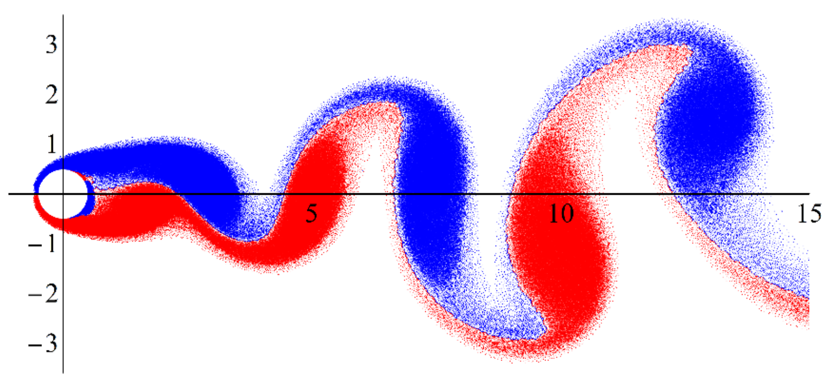

Figure 2: Vortex wake after circle cylinder.

Numerical experiments show that the usage of different schemes influences significantly the hydrodynamic loads acting on the airfoil. Values of unsteady drag and lift coefficients against time are shown in Fig. 3. It is seen that usage of the N-scheme provides rather high oscillation, so some special filtering procedure is required, while usage of the T-scheme provides much smaller amplitude of oscillations.

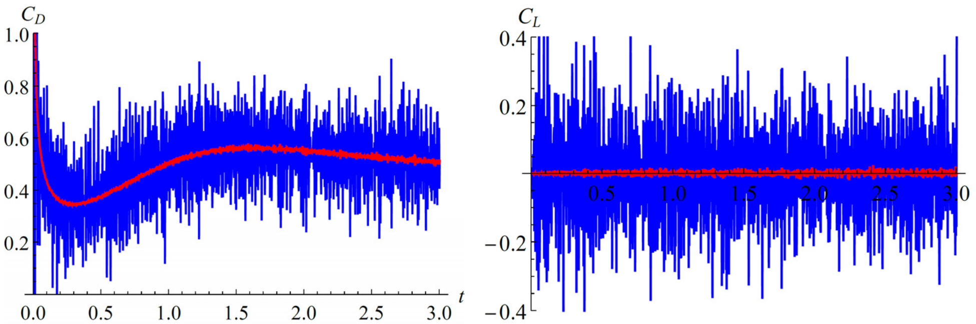

Figure 3: Hydrodynamic loads oscillations for flow simulation around impulsively started cylinder at Re = 200: N-scheme (blue) and T-scheme (red).

Another numerical experiment was performed for a similar problem at Re = 3,000. The drag coefficient for first 5 seconds is shown in Fig. 4 in comparison with results obtained by other authors [18]–[24]. A good agreement is observed. Results obtained by using VM2D are presented without any averaging.

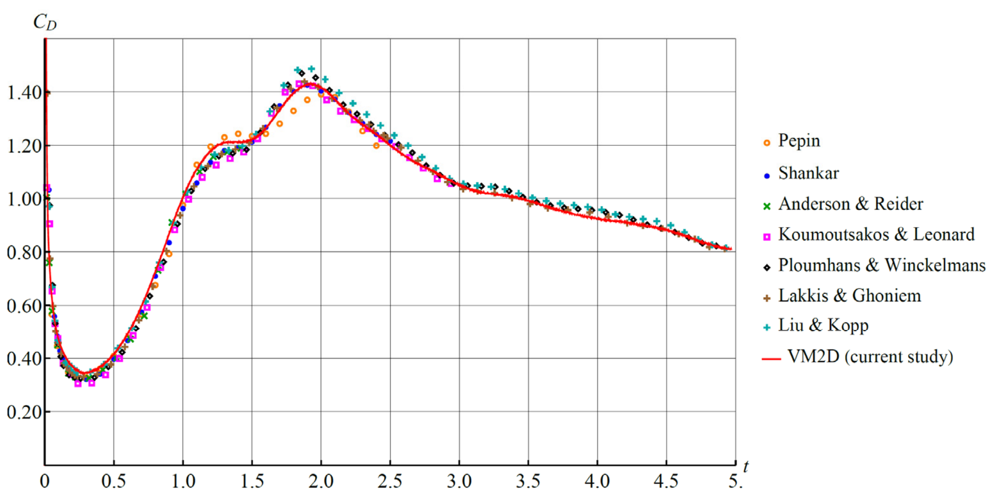

Figure 4: Unsteady drag coefficient for flow simulation around impulsively starting cylinder at Re = 3,000.

4.2 Flow around rectangular airfoil

The set if problems of flow simulation around rectangular airfoils with different chord to thickness ratio (c/t) is considered. Example of vortex wake in quasi-steady regime behind the rectangular airfoil with $c/t = 7$ is shown in Fig. 5 at Re = 400, which is calculated with respect to the thickness t.

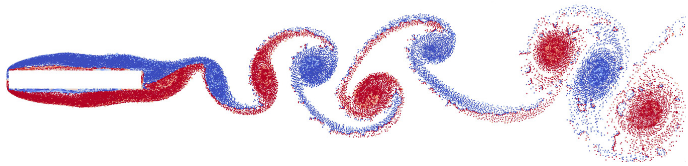

Figure 5: Vortex wake behind the rectangular airfoil.

For such set of problems an interesting effect can be observed. The Strouhal number calculated with respect to the airfoil chord is changing piecewise-constantly in dependence on the ratio c/t (Fig. 6). Numerical results are in a good agreement with results of other authors [24], [25].

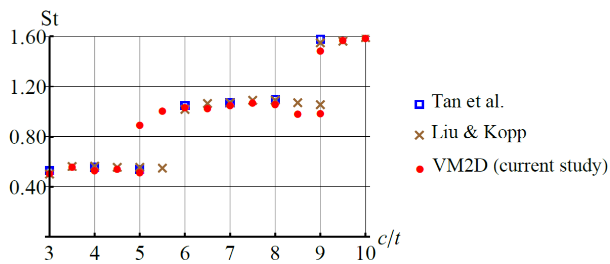

Figure 6: The Strouhal number against chord to thickness ratio.

4.3 Flow simulation around sphere

In VM3D for BIE solving the T-scheme with a piecewise-constant solution representation on triangular panels is implemented as well as a special algorithm of the solution correction to provide its divergence-free, based on the recovery of the double-layer potential density. The model problem of flow simulation around the sphere with unit diameter is considered. The surface is discretized by triangle panels of approximately equal areas. The steady regime of flow simulation is shown in Fig. 7.

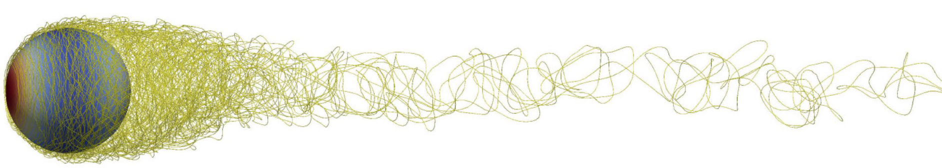

Figure 7: Vortex wake after the sphere.

Results of the computed averaged dimensionless pressure coefficient in dependence on the azimuthal angle of a point on the sphere are in good agreement with the experimental data as shown in Fig. 8.

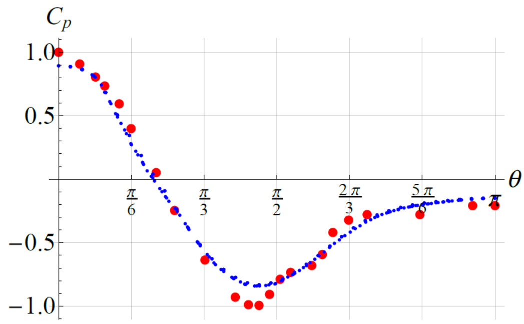

Figure 8: Dimensionless pressure coefficient against on the azimuthal angle: numerical experiment (blue points) and experimental data (red points).

4.4 Added masses calculation

For FSI problems different coupling schemes are known. The simplest weakly-coupled approach is the splitting scheme: hydrodynamic step of flow simulation for the surface motion according to the known law, and mechanic step for the surface motion under known forces. Note that if we deal with light body or airfoil such an approach leads to numerical instability. To overcome this problem strongly-coupled monolithic approach can be used when parameters of the vorticity and surface velocity are computed during single system solving. This scheme is more complicated to implement and is not universal, so an iterative semi-implicit scheme [26] is preferable, which requires a preliminary calculation of the necessary components of the added mass tensor.

Components of the matrix of added masses can be expressed through the solution of the BIE (intensity of the vortex sheet on the surface) during the solution of the set of problems: impulsive start of the body/airfoil with unit velocity along all 2 or 3 axes and its impulsive rotation with a unit angular velocity around all the axes. In fact it is necessary to perform only one time step for each problem.

In the 2D case matrix of the added mass tensor consist of six components. Let's consider the problem of added mass computation for the Zhukovsky wing airfoil (Fig. 9) since the exact solution is known.

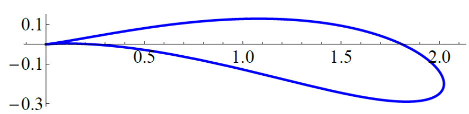

Figure 9: Zhukovsky airfoil shape.

Maximal relative errors are shown for all the components of the added mass tensor for a different number of panels are shown in Table 1, where three different numerical schemes are considered: *N*-scheme of the discrete vortex method and *T*-schemes with piecewise-constant (with index 0) and piecewise-linear (with index 1) solution representation.

Table 1: Relative errors of the added masses tensor estimation for the wing airfoil.

Number of panels	*N*-scheme	T^0-scheme	T^1-scheme
50	$3.4 \cdot 10^{-1}$	$5.7 \cdot 10^{-2}$	$1.7 \cdot 10^{-2}$
100	$6.2 \cdot 10^{-2}$	$2.5 \cdot 10^{-2}$	$4.6 \cdot 10^{-3}$
200	$3.9 \cdot 10^{-2}$	$1.3 \cdot 10^{-2}$	$1.7 \cdot 10^{-3}$
400	$2.2 \cdot 10^{-2}$	$6.9 \cdot 10^{-3}$	$7.4 \cdot 10^{-4}$
800	$1.2 \cdot 10^{-2}$	$3.7 \cdot 10^{-3}$	$3.5 \cdot 10^{-4}$
1,600	$6.1 \cdot 10^{-3}$	$2.0 \cdot 10^{-3}$	$1.7 \cdot 10^{-4}$
3,200	$3.4 \cdot 10^{-3}$	$1.1 \cdot 10^{-3}$	$8.5 \cdot 10^{-5}$

All the schemes provide close to the first order of accuracy. It is connected with exact solution behaviour in the *x*-directed motion the solution is bounded and has the first kind discontinuity at the cusp, however, for the *y*-directed motions the exact solution has a weak singularity at the cusp point. Values of added masses corresponding to the *x*-direction are calculated with the second order of accuracy when using the T^1-scheme. Note that in order to achieve an error level less than 1% for the *N*-scheme the airfoil should be discretized by 950 panels, while for T^0-scheme by 265 and for T^1-scheme by only 66 panels. For providing error level less than 0.1% it is required 10,800 panels for *N*-scheme, and 3,700 and only 307 for *T*-schemes respectively.

In 3D case, the problem of a three-axial ellipsoid is considered. It is known that for ellipsoid in principal axes, that are co-directional with its own axes, coefficients of added masses (λ_{11}, λ_{22}, λ_{33}) and coefficients of the added moments of inertia (λ_{44}, λ_{55}, λ_{66}) can be calculated exactly [27]. Relative errors of all components of the added mass tensor are given in Table 2 for ellipsoid with semiaxes $a = 0.5$, $b = 1.0$ and $c = 1.5$ discretized by triangle close to uniform mesh. For the BIE solving the *T*-scheme with piecewise-constant solution representation is used.

Table 2: Relative errors of added mass coefficients for ellipsoid.

Number of panels	$\delta\lambda_{11}$	$\delta\lambda_{22}$	$\delta\lambda_{33}$	$\delta\lambda_{44}$	$\delta\lambda_{55}$	$\delta\lambda_{66}$
186	0.1285	0.0713	0.0726	0.1081	0.2384	0.3200
488	0.0495	0.0275	0.0278	0.0420	0.1082	0.1427
954	0.0238	0.0151	0.0148	0.0248	0.0527	0.0699
2,060	0.0123	0.0064	0.0069	0.0093	0.0238	0.0338
3,780	0.0051	0.0045	0.0044	0.0066	0.0092	0.0126
7,780	0.0031	0.0017	0.0021	0.0017	0.0055	0.0088

It can be seen that the error decreases quite quickly with increasing of the number of panels; close to second order of accuracy is observed.

5 CONCLUSION

The present paper describes parallel open-source codes VM2D and VM3D are developed for the simulation of two- and three-dimensional viscous incompressible flows simulation around airfoils and bodies. *T*-schemes based on the Galerkin approach are developed and implemented for the numerical solution of the boundary integral equation. Test results show good agreement with the experimental data and other authors' results. At the same time, significantly lower level of non-stationary hydrodynamic loads oscillations can be observed in comparison with well-known *N*-schemes. The developed models and algorithms are suitable for numerical simulation in coupled FSI problems, including for light movable bodies/airfoils. Iterative semi-implicit approach is implemented, for which added masses tensor is calculated with rather high accuracy. Parallel implementation is performed using OpenMP, MPI and Nvidia CUDA technologies. The GPU-implementation is especially effective – one graphics accelerator Tesla V100 in terms of performance in VM2D can replace 84 28-core CPU nodes. There is also an opportunity to use several GPUs in parallel mode during one simulation, but it is not very efficient.

REFERENCES

[1] Kempka, S.N., Glass, M.W., Peery, J.S., Strickland, J.H. & Ingber, M.S., Accuracy considerations for implementing velocity boundary conditions in vorticity formulations. SANDIA Rep., SAND96-0583, 1996.
[2] Belotserkovsky, S.M. & Lifanov, I.K., *Method of Discrete Vortices*, CRC Press: New York, 464 pp., 1993.
[3] Marchevsky, I.K., Sokol, K.S. & Izmailova, I.A., *T*-schemes for mathematical simulation of vorticity generation on smooth airfoils in vortex methods. *Herald of the Bauman Moscow State Technical University, Series Natural Sciences*, **6**(105), 2022. (In Russian.)
[4] Chorin, A.J., Numerical study of slightly viscous flow. *Journal of Fluid Mechanics*, **57**, pp. 785–796, 1973.
[5] Degond, P. & Mas-Gallic, S., The weighted particle method for convection-diffusion equations. I. The case of an isotropic viscosity. *Mathematics of Computation*, **53**(188), pp. 485–507, 1989.
[6] Shankar, S. & van Dommelen, L., A new diffusion procedure for vortex methods. *J. Comput. Phys.*, **127**, pp. 88–109, 1996.
[7] Dynnikova, G.Y., The Lagrangian approach to solving the time-dependent Navier–Stokes equations. *Doklady Physics.*, **49**(11), pp. 648–652, 2004.
[8] Mimeau, C. & Mortazavi, I., A review of vortex methods and their applications: From creation to recent advances. *Fluids*, **6**, 68, 2021.
[9] Lifanov, I.K., *Singular Integral Equations and Discrete Vortices*, VSP: Utrecht, 475 pp., 1996.
[10] Lewis, R.I., *Vortex Element Methods for Fluid Dynamic Analysis of Engineering Systems*, Cambridge University Press: Cambridge, UK, 566 pp., 1991.
[11] vvflow: CFD software for performing flow simulations with viscous vortex domains (VVD) method. https://github.com/vvflow. Accessed on: 29 Jun. 2023.
[12] Omega2D: Two-dimensional flow solver with GUI using vortex particle and boundary element methods. https://github.com/Applied-Scientific-Research/Omega2D. Accessed on: 29 Jun. 2023.
[13] Omega3D: 3D flowsolverwith GUI using vortex particle and boundary element methods. https://github.com/Applied-Scientific-Research/Omega3D. Accessed on: 29 Jun. 2023.
[14] FLOW Unsteady Aerodynamics Suite. https://github.com/byuflowlab/FLOWUnsteady. Accessed on: 29 Jun. 2023.
[15] Chair of Modelling and Simulation of Structures, Prof. Dr. Guido Morgenthal. https://www.uni-weimar.de/en/civil-engineering/chairs/modelling-and-simulation-of-structures/software/. Accessed on: 29 Jun. 2023.

[16] Ryatina, E. & Lagno A., The Barnes–Hut-type algorithm in 2D Lagrangian vortex particle methods. *J. Phys.: Conf. Ser.*, **1715**, 012069, 2021.
[17] Ryatina, E., Marchevsky, I. & Kolganova A., Boundary integral equation solving in vortex method using the Barnes–Hut/multipole algorithm. *Proceedings of the 2022 Ivannikov Ispras Open Conference (ISPRAS)*, pp. 74–80, 2022.
[18] Pepin, F.M., Simulation of the flow past an impulsively started cylinder using a discrete vortex method. PhD thesis, California Institute of Technology, 1990.
[19] Shankar, S., A new mesh-free vortex method. PhD thesis, FAMU-FSU College of Engineering, Florida, 1996.
[20] Anderson, C.R., Vorticity boundary conditions and boundary vorticity generation for two-dimensional viscous incompressible flows. *J. Comput. Phys.*, **80**, pp. 72–97, 1989.
[21] Koumoutsakos, P. & Leonard, A., High-resolution simulations of the flow around an impulsively started cylinder using vortex methods. *J. Fluid Mech*., **296**, pp. 1–38, 1995.
[22] Ploumhans, P. & Winckelmans, G.S., Vortex methods for high-resolution simulations of viscous flow past bluff bodies of general geometry. *J. Comput. Phys*., **165**(2), pp. 354–406, 2000.
[23] Lakkis, I. & Ghoniem, A., A high resolution spatially adaptive vortex method for separating flows. Part I: Two-dimensional domains. *J. Comput. Phys*., **228**(2), pp. 491–515, 2009.
[24] Liu, Z. & Kopp, G.A., High-resolution vortex particle simulations of flows around rectangular cylinders. *Comp. Fluids.*, **40**, pp. 2–11, 2011.
[25] Tan, B.T., Thompson, M.C. & Hourigan, K., Simulated flow around long rectangular plates under cross flow perturbations. *Int. J. Fluid Dyn*., **2**, 1, 1998.
[26] Dynnikova, G.Y., Added mass in a model of a viscous incompressible fluid. *Doklady Phys*., **64**, 397–400, 2019.
[27] Korotkin, A.I., *Added Masses of Ship Structures*. Series: Fluid Mechanics and its Applications, Vol. 88, Springer, 391 pp., 2009.